Optimal design of IPM-PMASR motors for wide constant power speed range applications

Proceedings of
11th European Conference on Turbomachinery Fluid dynamics & Thermodynamics
ETC11, March 23-27, 2015, Madrid, Spain

EXPERIMENTAL AND NUMERICAL EVALUATION OF THE $NPSH_R$ CURVE OF AN INDUSTRIAL CENTRIFUGAL PUMP

S. Salvadori[*a] *- A. Cappelletti*[*] *- F. Montomoli*[¶] *- A. Nicchio*[§] *- F. Martelli*[*]

[*] Department of Industrial Engineering, University of Florence
via di S. Marta, 3 - 50139, Florence, Italy

[¶] Imperial College
SW7 2AZ, London, UK

WEIR Gabbioneta srl
[§] viale Casiraghi, 68 - 20099, Sesto S. Giovanni, Milan, Italy

ABSTRACT

Cavitation triggers harmful flow instabilities yielding both significant decrease of performance and reduced reliability. The aim of this paper is to investigate the accuracy of numerical methodologies for the correct prediction of cavitation inception in centrifugal pumps. Preliminary analyses are performed on the NACA 0009 hydrofoil using the ANSYS CFX V14.5 code. The available bubble dynamics model is calibrated using the experimental data in cavitation conditions. Then, the optimized parameters are used for the evaluation of the $NPSH_R$ curve of the R250 centrifugal pump industrial pump designed by WEIR-Gabbioneta srl. Reynolds-Averaged Navier-Stokes mono- and two-phase calculations are performed. The performance curve of the R250 centrifugal pump is evaluated at first, and then the $NPSH_R$ curve is obtained for the design flow rate. The control volume of the numerical analysis includes all the hydraulic features from flange to flange (except for the side chambers) and then a direct comparison with the available experimental data obtained during two experimental campaigns is possible. The numerical activity demonstrated that an adequately calibrated model is able to reproduce the shape of the cavitation curve of an industrial centrifugal pump, although the $NPSH_R$ value is underestimated.

NOMENCLATURE

BD		Bubble Dynamics
BEP		Best Efficiency Point
BT		Barotropic
C_{ax}	[m]	axial chord
CFD		Computational Fluid Dynamics
C_p	[-]	pressure coefficient
D	[m]	impeller outlet diameter
FR		Frozen Rotor
G	[m/s^2]	gravity acceleration
H	[m]	head
k	[m^2/s^2]	turbulent kinetic energy
KERNG		k-ε Renormalized Group
N	[RPM]	rotational speed
$NPSH_R$	[m]	Required Net Positive Suction Head
n_b		bubble number density
n_s	[$m^{3/4}/s^{3/2}$]	specific speed
p	[Pa]	local pressure
p_{01}	[Pa]	stagnation pressure at the pump inlet section
p_{ref}	[Pa]	reference pressure

[a] contact author: office +39 055 2758 779, email simone.salvadori@unifi.it

p_{sat}	[Pa]	saturation pressure
Q	[m^3/s]	flow rate
R_b	[m]	bubble radius
$\dot{S}$		net phase change rate
SST		Shear Stress Transport
UNIFI		University of Florence
UNIPD		University of Padova
U_{ref}	[m/s]	reference velocity
VoF		Volume of Fluid
x	[m]	axial coordinate
y^+	[-]	dimensionless wall distance
α_{vap}		vapor volume fraction
ε	[m^2/s^3]	turbulence dissipation rate
ρ_l	[kg/m^3]	liquid phase density
σ	[-]	cavitation number
Φ	[-]	flow coefficient
Ψ	[-]	head coefficient
ω	[1/s]	specific turbulence dissipation rate

INTRODUCTION

Cavitation is a paramount issue for pump designers. Its development is responsible for noise production and damage of the impeller surfaces. Under certain working conditions, fluid pressure decreases under the saturation value and bubbles appear. Due to the density step between the two phases, steam volume is much higher than the corresponding water volume. Bubbles move toward the exit section driven by the positive pressure gradient. Then, implosion occurs and the surfaces are continuously subject to tough forces. This phenomenon is called "pitting" and it is responsible for pump mechanical deterioration. Also the pump performances are affected by cavitation insurgence, since both head and efficiency decrease when bubbles appear.

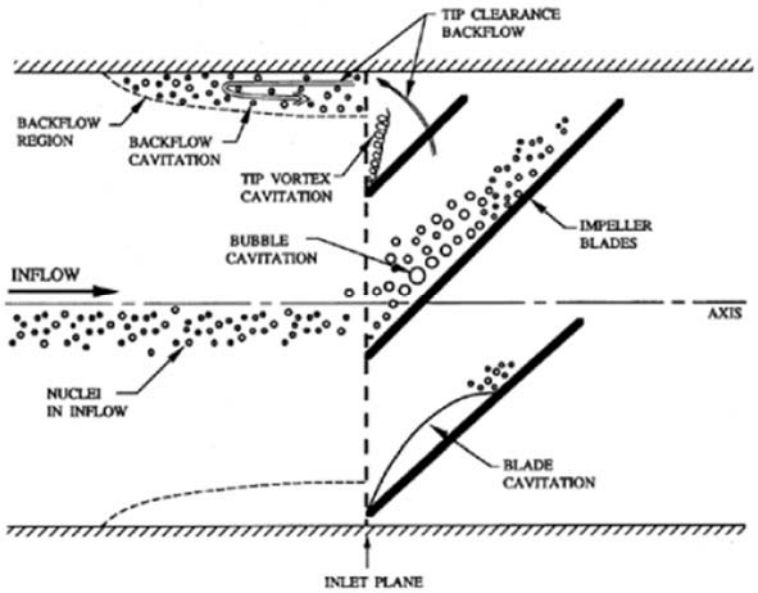

Figure 1 Classification by Brennen (1994)

Although the change of phase is always correlated to the pressure decrease, cavitation appears in several sections with many modalities. Brennen (1994) proposed the classification reported in Figure 1. The most common cavitation insurgence is related to the flow acceleration on the blade suction side. This case is called “blade cavitation” and can be divided into two sub-categories. “Partial cavitation” occurs whenever bubbles collapse on the suction side of the blade. This is the most dangerous case due to the pitting occurrence. “Supercavitation” occurs when bubbles collapse

in the region downstream of the blade trailing edge. The main advantage of the latter case is that the pitting is neglected as well as the surface damage.

Predicting "partial cavitation" is clearly a key aspect of pump design. The available computational resources allow evaluating cavitation using numerical models implemented in state-of-the-art Computational Fluid Dynamics (CFD) codes. According to the classification proposed by Tamura and Matsumoto (2009), the numerical approaches can be divided into two main groups: the interface tracking methods, like Volume of Fluid (VoF) methods (Kunz et al. (1999)), and the continuum modeling. The latter can be divided into two sub-groups: the Barotropic (BT) methods (Delannoy and Kueny (1990)) and the Bubble Dynamics (BD) methods (Singhal et al. (2001), Schnerr and Sauer (2001), Zwart et al. (2004)).

In this work, the BD family of approaches is considered. BD methods are able to evaluate both accumulation and collapse of the bubbles. A simplified version of the Rayleigh-Plesset equation, where the slip velocity between the fluid and the bubbles is neglected, is used to model the mass transport between the phases. For this reason, these methods can be used in a wide range of cases, except for cases with very large void fractions. In fact, the main drawback of the BD methods is that bubble-bubble interactions are neglected and a large steam portion generates numerical instability. It is the author's opinion that amongst the BD methods, the algorithms proposed by Singhal et al. (2001), Schnerr and Sauer (2001) and Zwart et al. (2004) are the most interesting. A detailed description of the methods can be found in the cited papers while the main characteristics are listed below. All these methods use the same steam transport equation and the same bubble dynamics considerations. These methods differ by the definition of the vapor volume fraction α_{vap} and of the net phase change rate $\dot{S}$. The bubble number density n_b represents the number of bubbles per unit volume and is the key parameter for those methods. The evaluation of n_b can be performed numerically once the local values of density, pressure, α_{vap} and bubble radius R_b are available (Equation 1).

$$n_b = \frac{\alpha_{vap}}{\frac{4}{3}\pi R_b^3} \tag{1}$$

The methods by Singhal and by the Schnerr also take into account the densities of both the phases and of the mixture to evaluate R_b. The Zwart model considers the vapor density only, and is simple to implement in its baseline form. One of the main limits of both the Schnerr and the Zwart methods is that they do not take into consideration the incondensable gases in the basic model terms, while Singhal model does it.

The authors decided to test the reliability of BD cavitation models when studying an industrial centrifugal pump where a large void fraction is not expected. The numerical campaign has been realized using the ANSYS CFX V14.5 code, equipped with a modified version of the model proposed by Zwart et al. (2004). The paper is divided into two main sections: in the first part the BD model parameters are tuned using the pressure coefficient over a NACA 0009 profile in cavitating conditions. In the second part of the paper the most promising set of parameters is used for the evaluation of the $NPSH_R$ of a centrifugal pump.

ASSESSMENT OF THE NUMERICAL MODEL

The aim of this part of the work is to analyze, in terms of accuracy and numerical stability, the cavitation model already available in the ANSYS CFX V14.5 commercial CFD code. Model parameters are modified to tune the model using the available experimental data. The selected test case is the NACA 0009 hydrofoil mounted into a square-section channel and invested by a water flow, both in non-cavitating and cavitating conditions. The profile is characterized by a maximum thickness of 10 mm and is truncated for mechanical reasons at 90% of the chord. Salvadori et al.

(2012) already described some aspects of the present validation and then only a brief description is reported here.

Numerical approach

The experiments were simulated in ANSYS CFX V14.5 using a two-dimensional computational domain that reproduces the mid-section of the water tunnel. The grid used for the simulations is shown in Figure 2. It is composed by a first one, structured, adjacent to the inlet section and a second one, hybrid unstructured, in which the NACA 0009 profile is located, with an angle of attack of 2.5 degrees. The zones are joined by a grid interface. Special attention was posed in the dimension of the elements facing with each other in the boundary layer and the free stream zones. The extension of the domain upstream of the profile has been created to allow the boundary layer development on the end-walls before the leading edge of the hydrofoil. Particular attention was posed in the discretization of the leading edge and of the suction side. In fact, their influence on the bubble development is crucial and a local refinement was realized. Along the profile ten prismatic layers were posed and the width of the first layer was chosen in order to obtain y^+ around 1. The whole grid is composed by about 300,000 elements.

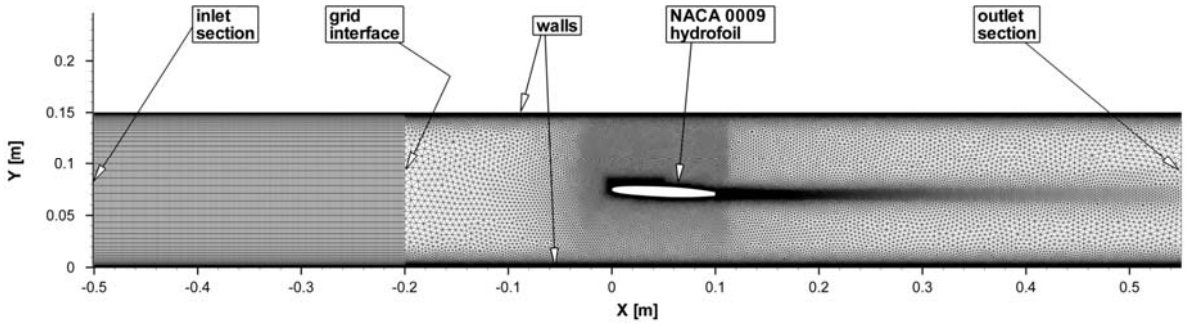

Figure 2 Computational mesh for the NACA 0009 hydrofoil

The full set of Reynolds-averaged Navier-Stokes equations were solved with the assumptions of a steady flow. The SST model by Menter (1992) has been used to take into account the effects of turbulence. A second-order scheme has been considered for the momentum equations while a first-order scheme has been used for turbulence and vapor transport equations. The inlet velocity (20 m/s) and the outlet pressure have been specified as boundary conditions. On both end-walls and hydrofoil surface no-slip conditions were imposed. For what concerns the turbulence scalar quantities, the inlet turbulence intensity is 5% and a turbulence length scale of 0.00375 m. This last value has been calculated considering 1/20 of the mid-height of the channel.

For the cavitation prediction the built-in BD model by Bakir et al. (2004) has been considered. A test performed by on the same mesh Marini et al. (2011) using the BD models implemented in the ANSYS Fluent V13 shows that the model by Zwart et al. (2004) is the most accurate when standard parameters are considered. As in the paper by Marini et al. (2011), the analysis in cavitation conditions are performed with a constant cavitation number σ (defined as reported in Equation 2) of 0.81 which corresponds to a saturation pressure p_{sat} of 3540Pa. Inlet pressure and velocity were selected as reference values.

$$\sigma = \frac{p_{ref} - p_{sat}}{\frac{1}{2}\rho_l U_{ref}^2} \tag{2}$$

A single-phase simulation has been performed to validate the numerical approach, including grid effects. Then, eleven simulations have been performed changing the parameters of the cavitation model. Amongst them, results obtained from the most promising simulations are reported here. Parameters are reported in Table 1: since the bubble number density cannot be directly

modified in ANSYS CFX V14.5, the vapor volume fraction α_{vap} and the mean bubble radius R_b are modified and then n_b recalculated. The relation between n_b, α_{vap} and R_b is reported in Equation 1. Convergence was monitored taking into account the residuals and the mass imbalance. The calculations were considered converged once all the parameters were lower than 10^{-6} and almost constant over the numerical iterations.

Table 1 Test matrix for the NACA 0009 profile

ID	n_b	R_b	α_{vap}
0	-	-	-
1 (default)	10^{14}	10^{-6}	$5*10^{-4}$
2	10^{15}	10^{-6}	$4*10^{-3}$
3	$7.64*10^{15}$	$0.25*10^{-6}$	$5*10^{-4}$
4	10^{17}	10^{-6}	$5*10^{-1}$

Results

Results obtained from the numerical simulations are compared with each other and with the available experimental data from Dupont (1991). Results are presented in terms of pressure coefficient C_p (Equation 3), calculated with respect to reference taken values at the inlet section.

$$C_p = \frac{p - p_{ref}}{\frac{1}{2}\rho_l U_{ref}^2} \tag{3}$$

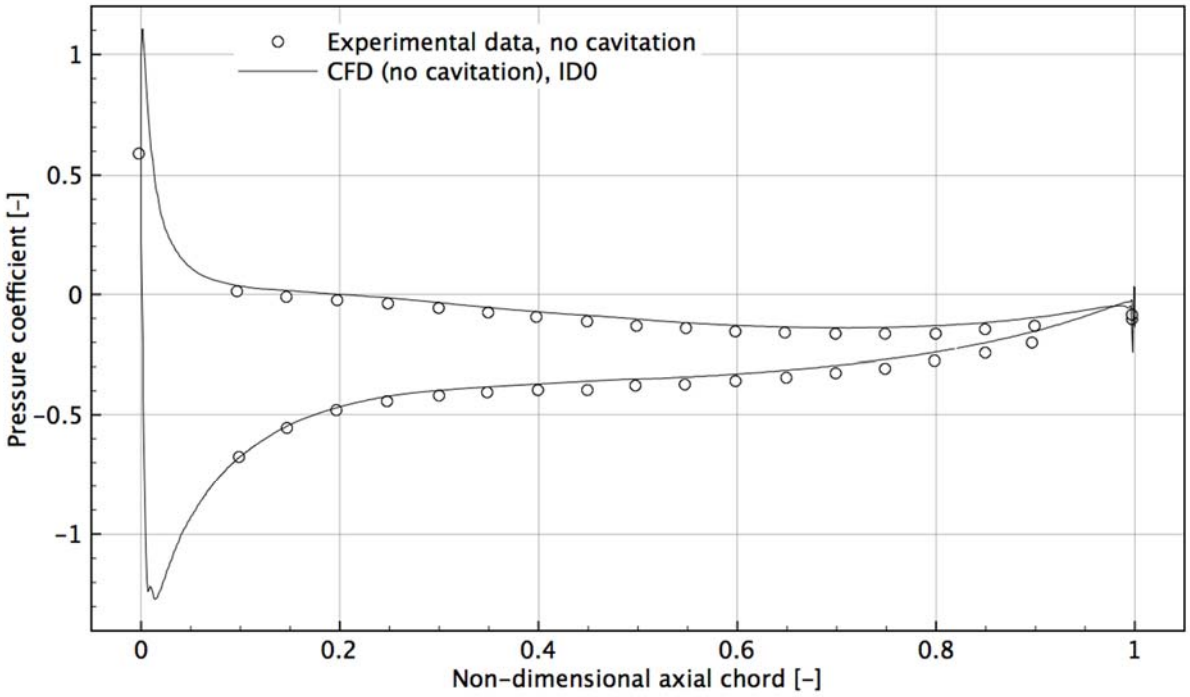

Figure 3 Pressure coefficient along the NACA 0009 profile: single-phase

Figure 3 shows the comparison between experimental and numerical data for the single-phase case. There is a good agreement between CFD and experiments along the entire hydrofoil except for the trailing edge region, where an overestimation of the base pressure is visible. It must be underlined that the disagreement is very limited and that the miss-prediction of the base region is a classical outcome of steady calculations.

Figure 4 shows results for the multi-phase case with $\sigma = 0.81$. The separation bubble generated by cavitation starts at $x/C_{ax} = 0.25$ and is closed approximately at $x/C_{ax} = 0.60$. It can be immediately observed that the original model (ID1) is not able to correctly reproduce the phenomenon while modified models show an increased accuracy. Amongst them, model ID2 is able to reproduce correctly the C_p behavior along the entire hydrofoil and then it has been chosen for the subsequent analysis of the R250 centrifugal pump.

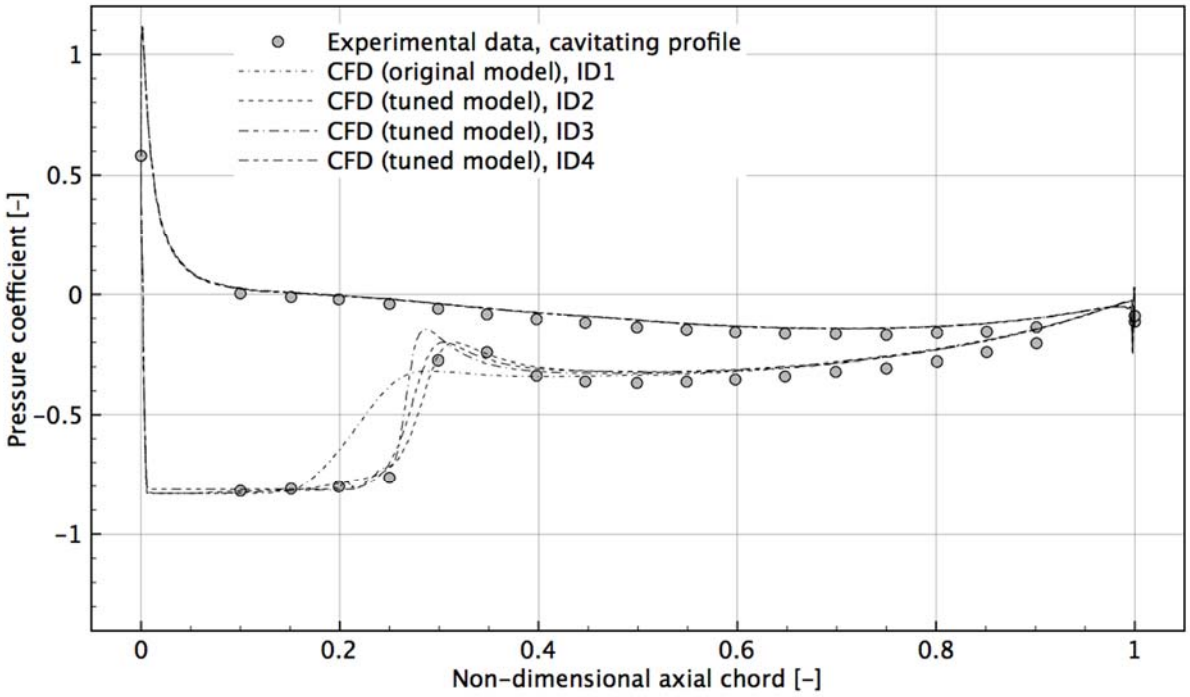

Figure 4 Pressure coefficient along the NACA 0009 profile: multi-phase

SIMULATION OF THE R250 CENTRIFUGAL PUMP

The R250 centrifugal pump is a single stage centrifugal pump characterized by a low n_s developed by WEIR-Gabbioneta srl. It has been experimentally tested both by the designers and in a test rig located at the University of Padova (UNIPD).

Numerical approach

Control volume for the numerical simulation includes all the hydraulic features of the test bench located at the WEIR-Gabbioneta srl headquarters, except for the side chambers. The aim of the activity is to perform CFD simulation "from flange to flange" and then to analyze the flow field inside of all the components. The control volume includes the feeding duct (Figure 5a), the impeller and the volute (Figure 5b) and a discharge duct of conical shape (Figure 5c). The inlet and outlet sections of the control volume are positioned in correspondence of the rakes of pressure taps of the experimental apparatus. The front and rear cavities of the impeller have partially included in the control volume but with zero leakage flow rates: the effect of this approximation will be discussed later in the text, where experimental and numerical results are compared.

The grid used for the simulations has been realized using the commercial grid generator Centaur and is shown in Figure 5. Special attention has been paid to the mesh quality on the interfaces between components: in particular, the interface between the impeller and the volute consists of a circumferential cylinder and two discs that lay on a plane orthogonal to the pump axis. That solution allows to taking into account the sudden variation of area occurring on that region. Particular attention has also been posed in the discretization of the impeller blade near the leading edge, where the bubble development occurs. Along the walls ten prismatic layers were posed and

the width of the first layer was chosen in order to obtain y^+ between 30 and 300. The whole grid is composed by about 6,500,000 elements.

In most of the cases the interfaces are treated using a mixing plane approach since the feeding duct do not have any mechanical component in proximity to the impeller blades. It must be underlined that the interaction between the volute tongue and the impeller blades has a severe impact on the cavitation insurgence, and then the frozen rotor approach has also been used for the reconstruction of the nominal $NPSH_R$ curve. Two relative positions between the volute tongue and the impeller blade have been considered, aligned and rotated by half pitch.

The SST model by Menter (1992) and the k-ε RNG by Yakhot et al. (1992) have been used to take into account the effects of turbulence. A second-order scheme has been considered for the momentum equations while a first-order scheme has been used for time integration, turbulence and vapor transport equations. The inlet flow rate and the outlet pressure have been specified as boundary conditions. No-slip conditions were imposed on the surfaces and the rotating condition has been used for the end-walls dealing to the impeller. For what concerns the turbulence scalar quantities, the inlet turbulence intensity is 1% and a turbulence length scale of 0.019 m. This last value has been calculated considering the channel diameter.

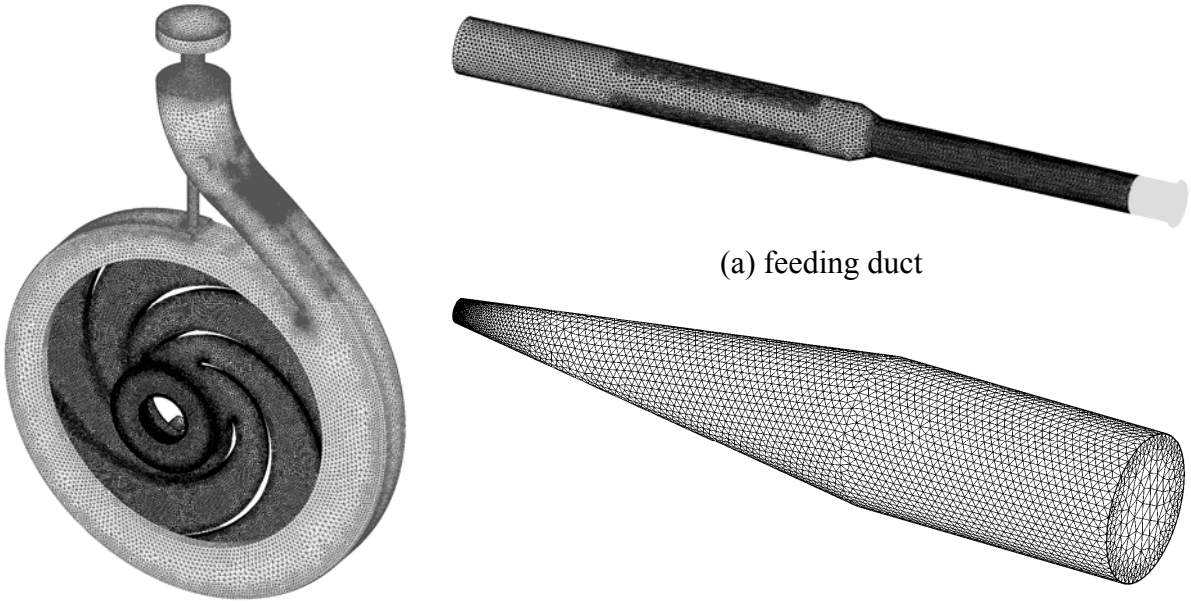

(a) feeding duct

(b) impeller and volute

(c) discharge duct

Figure 5 Computational mesh for the R250 pump

Table 2 Test matrix for the R250 pump

	σ [-]	Cavitation model	Turbulence model	Number of CFD simulations	$NPSH_{R,3\%}$ [m]
Performance	NA	NA	SST	6 (Stage)	NA
Cavitation	0.139	Tuned (ID 2)	SST	12 (Stage)	0.40
Cavitation	0.146	Tuned (ID 2)	SST	7 (Stage)	0.40
Cavitation	0.146	Original (ID 1)	SST	6 (Stage)	0.25
Cavitation	0.145	Tuned (ID 2)	k-ε RNG	8 (Stage)	0.40
Cavitation	0.145	Tuned (ID 2)	k-ε RNG	20 (FR)	1.00

Single-phase simulations have been initially performed to validate the numerical approach, including effects related to the grid density. The performance curve has been reconstructed considering the range of flow rates suggested by the pump designers. Then, a number of simulations

have been performed to reconstruct the $NPSH_R$ curve at BEP. For the cavitation prediction the built-in BD model by Bakir et al. (2004) has been considered. Simulations have been performed varying the saturation pressure, the cavitation model parameters (original and tuned) and the turbulence model. The full test matrix is reported in Table 2. Convergence was monitored taking into account the residuals and the mass imbalance. Calculations were considered converged once all the parameters were constantly lower than 10^{-4} and almost constant over the numerical iterations.

Performance

The comparison between the numerical results and the available experimental data is reported in Figure 6. Since there is no exact correspondence between the flow rates and between the rotational speeds analyzed during the two different experimental tests, results are presented in terms of flow coefficient (Equation 4) and head coefficient (Equation 5).

$$\phi = \frac{Q}{ND^3} \tag{4}$$

$$\psi = \frac{gH}{N^2D^2} \tag{5}$$

As can be observed in Figure 6 the agreement between CFD and experiments is satisfactory over all the considered range of flow rates, including extreme off-design conditions. Obtained results seem to suggest that the effect of the leakage flow rate are negligible, which is an unexpected results considering that the pump has a low specific speed. Then, an estimation of leakage flow rate has been performed using the dimensional curve of the impeller head, the geometrical characteristics of the clearances and a correlation by Stirling (1982).

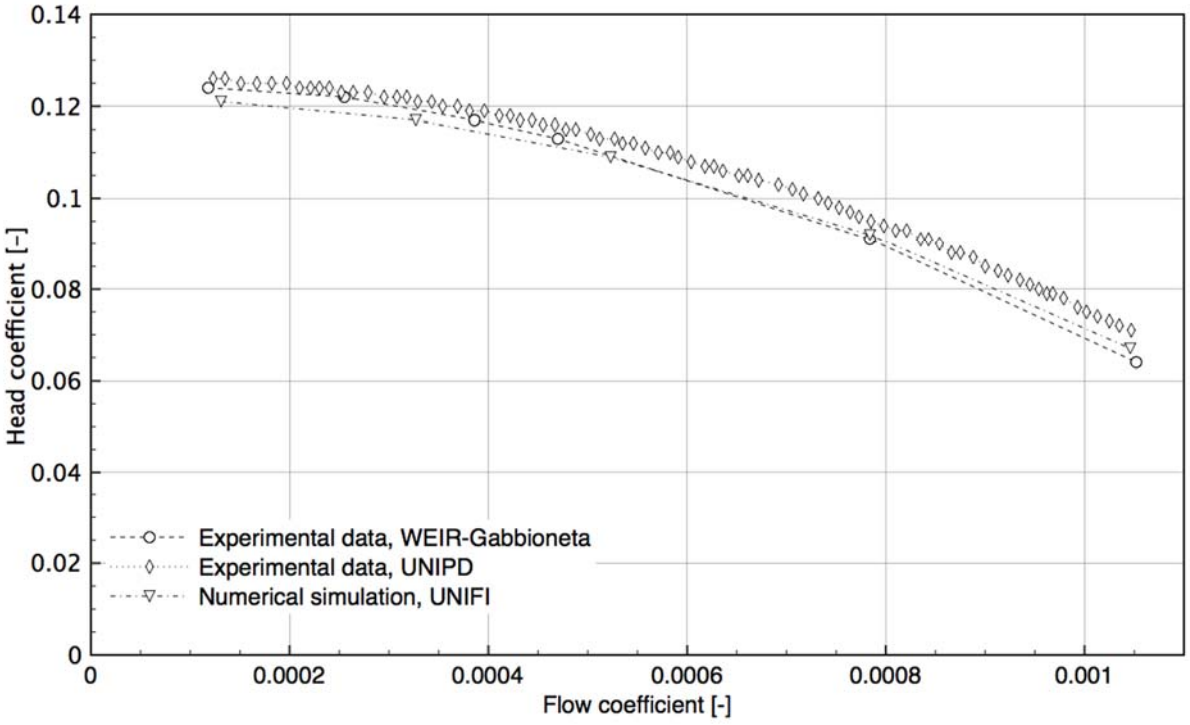

Figure 6 Performance curve of the R250 centrifugal pump

The leakage flow through each cavity has been initially evaluated using the experimental value of impeller head. Then, the new value of flow rate through the impeller is used to evaluate the impeller head using the performance curve. It must be underlined that this head value demonstrated

to be almost insensitive to the variation of the flow rate and then the procedure converged quickly. It has been observed that the flow rate through the impeller for the nominal conditions is nearly 36.9% higher than the nominal value (front cavity +22.6%, rear cavity +14.3%). Then, it cannot be said that leakage flows are negligible in terms of flow rate. However, impeller head is reduced by a very low factor (1.45%) and this explains why numerical results are so close to the experiments also neglecting side chambers. A similar result is not expected for the $NPSH_R$ curve since flow addiction in the inlet section and from the balancing holes have a severe impact on cavitation occurrence.

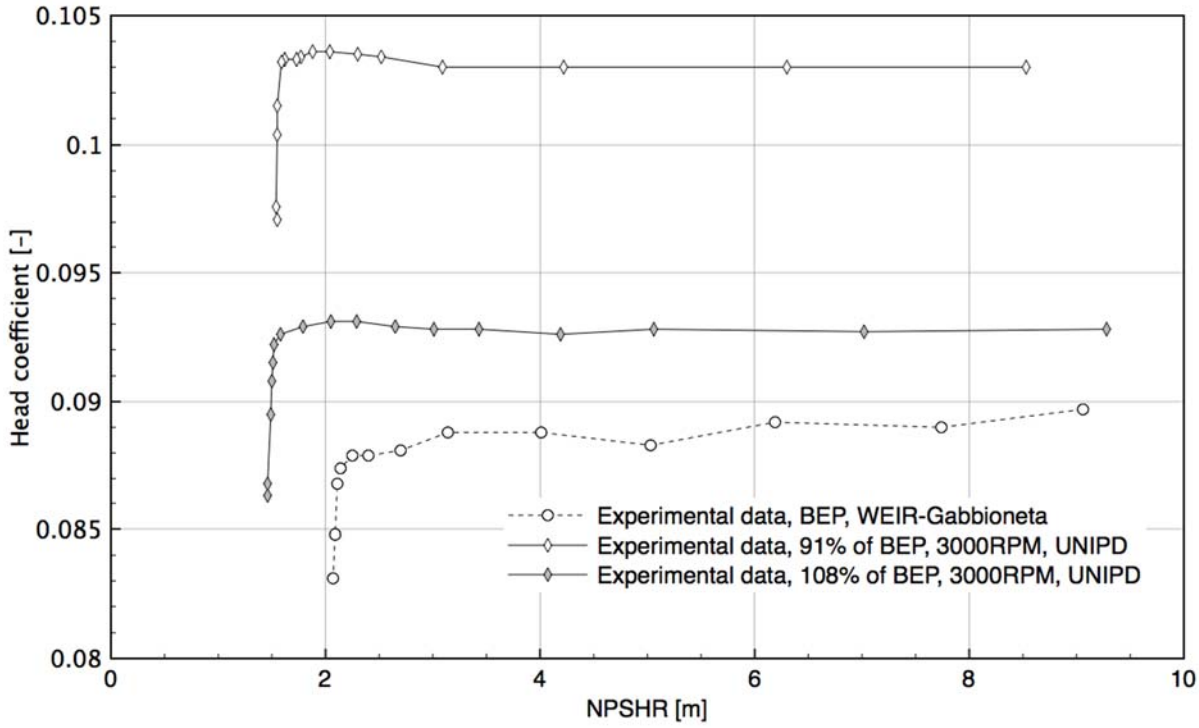

Figure 7 Cavitation curve, experimental data

Cavitation curve

In Figure 7 the comparison between the experimental results is reported. Results are presented in terms of $NPSH_R$ (Equation 6) and head coefficient (Equation 5). The $NPSH_R$ value obtained by UNIPD has been rescaled considering that $NPSH_R \propto N^{4/3} \cdot Q^{2/3}$ (Tuzson, 2000) to deal with the already cited difference in the experimental conditions. The $NPSH_{R,3\%}$ value is the one obtained for a head drop of 3% with respect to the no-cavitation head value.

$$NPSH_R = \frac{p_{01} - p_{sat}}{\rho_l \cdot g} \tag{6}$$

It can be observed that the no-cavitation head estimated by WEIR-Gabbioneta srl is slightly lower than the one reported in Figure 6 for BEP. This result can be explained considering that it is hard to repeat experimental tests in an industrial test rig designed to work with a very large range of machines. This is also evident when considering that the head value decreases when the suction head is decreased from 9 m to 2 m: this means that the flow rate is not exactly maintained, although the $NPSH_{R,3\%}$ value for BEP can be individuated around 2.07 m. Also UNIPD suggests similar $NPSH_{R,3\%}$ values: 1.55 m for 91% of BEP and 1.46 m for 108% of BEP.

From a numerical point of view it is possible to maintain unchanged the flow rate. The procedure used to reconstruct the cavitation curve consists in imposing the flow rate at the inlet section of the feeding duct and to reduce the pressure level at the outlet section of the discharge duct. Saturation pressure p_{sat} is based on the temperature of the incoming flow, which is indicated in

internal reports of the experimental campaign. Depending on the test, a different temperature value has been registered and then several cavitation curves have been evaluated varying σ. Numerical results are compared with experimental data in Figure 8. Although the flow rate is kept unchanged varying the outlet pressure, numerical results show a slightly higher value with respect to the single-phase analysis (Figure 6, +3%). Since none of the parameters have been changed except for the activation of the cavitation model, the latter can be considered as responsible for this decrease of accuracy in the evaluation of the pump head.

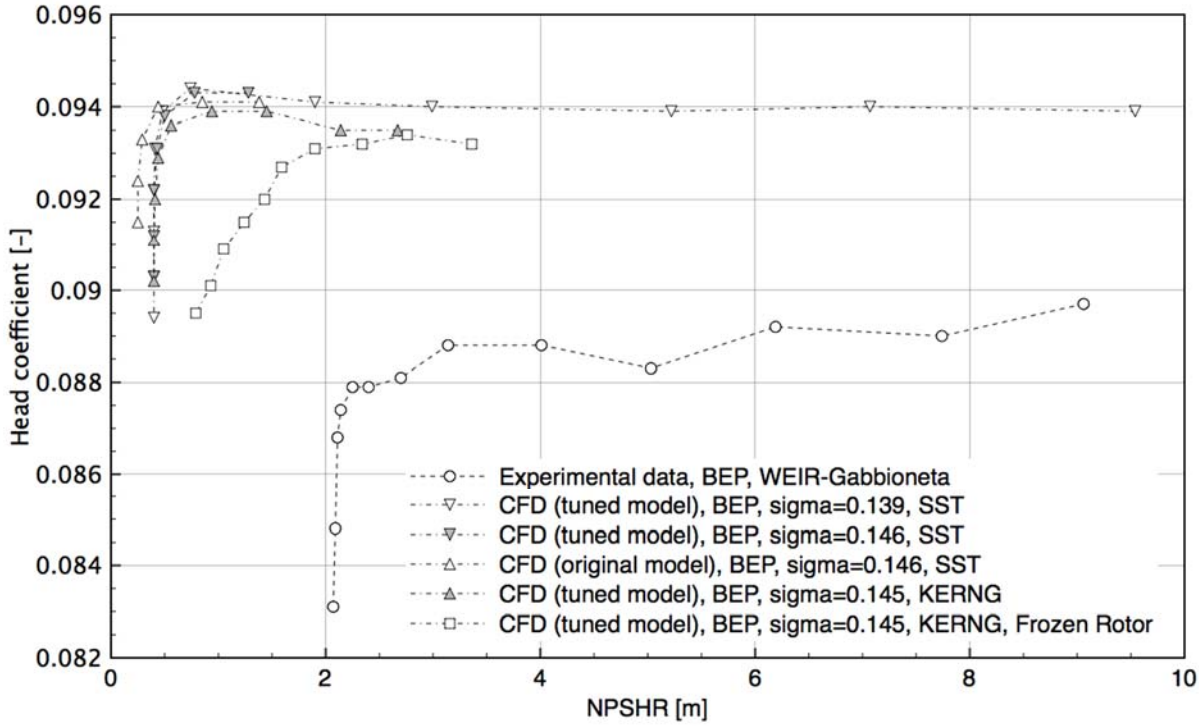

Figure 8 Cavitation curve, numerical results

Considering the curves evaluated by CFD using the mixing plane approach, it is clearly visible that $NPSH_{R,3\%}$ value is always underestimated. In fact, its value is 0.40 m when considering the tuned cavitation model and 0.25 m using the original model. No relevant effect has been individuated when changing the σ value. Changing the turbulence model modifies the value of the pump head in single-phase conditions but the underestimation of the $NPSH_{R,3\%}$ remains. Considering results obtained using the tuned model, CFD underestimates the $NPSH_{R,3\%}$ value of approximately 16,250 Pa. Although the $NPSH_{R,3\%}$ evaluation is not as accurate as expected it must be underlined that in terms of pressure the error represents only the 2.4% of the stagnation head of the impeller. Furthermore, it is well known that the mixing plane approach is not strictly conservative in terms of total pressure and then the evaluation of p_{01} for the calculation of the $NPSH_R$ value is affected by the interface treatment. Nevertheless the method seems to be accurate to reproduce the shape of the cavitation curve, it could provide more accurate results when considering either a pump with higher n_s values or a different approach for interfaces.

Considering the curve obtained using the frozen rotor approach, it can be observed that the predicted $NPSH_{R,3\%}$ is around 1.00 m. That value is much higher than the ones obtained using the mixing plane approach and the underestimation with respect to the experimental data is reduced to 10,400 Pa (1.5% of the stagnation head of the impeller). On the other side, the shape of the cavitation curve is not well reproduced. Although a region of constant head coefficient is clearly visible, the knee of the curve is smoothed and the $NPSH_R$ value keeps reducing when the inlet stagnation pressure is reduced. That result could be generated by the averaging procedure between two clocking position. In addition, the number of relative positions between the impeller blades and

the volute tongue could be too low for an accurate prediction of the cavitation phenomenon. However, looking at the obtained results it cannot be concluded that the frozen rotor approach is globally more accurate than the mixing plane approach.

CONCLUSIONS

The bubble dynamics model for cavitation analysis implemented in the commercial CFD tool ANSYS CFX 14.5 has been tuned using the experimental data of the NACA 0009 hydrofoil. The obtained set of model parameters has been used to determine the cavitation curve of the industrial centrifugal pump R250 by WEIR-Gabbioneta srl. Although correlations suggest that leakage flows represent 36.9% of the flow rate through the impeller at BEP, numerical results show that a good agreement can be obtained in terms of performance of the pump in single-phase conditions.

Cavitation phenomenon has been studied using both mixing plane and frozen rotor approaches for stage coupling. The effect of the model parameters, of the saturation pressure and of the turbulence model has been also analyzed. It must be underlined that a non-negligible underestimation of $NPSH_{R,3\%}$ is individuated using both the models. Considering the mixing plane results, the tuned model works better than the original one while no effect of either the turbulence model or the saturation pressure has been individuated. The shape of the cavitation curve has been well reproduced but an underestimation of approximately 1.60 m has been individuated. It can be observed that it corresponds approximately to 16,250 Pa, which is around 2.4% of the stagnation head of the impeller. That level of approximation is usually accepted in the numerical analysis of complex flows. Mixing plane approach could also have an impact in the analysis of $NPSH_R$ value since it affects the evaluation of the stagnation pressure at the impeller inlet section. Frozen rotor performs better in terms of $NPSH_{R,3\%}$ (the underestimation is limited to 1.07 m) but the curve shape is somehow smoothed.

One of the conclusions of this work is that both mixing plane and frozen rotor approaches do not provide satisfactory results for the present pump. The use of a more realistic coupling methodology (i.e. full unsteady) and the injection of the leakage flow rate at the impeller inlet section could improve the accuracy of the numerical method. The application of the presented methodologies to a pump characterized by a higher n_s could also provide information on the limitations of the selected approaches.

ACKNOWLEDGEMENTS

Present activity has been performed in the frame of the MOCAP project funded by the Region of Tuscany (funding scheme POR CRO FSE 2007-2013, UNIFI_FSE2012) and supported by WEIR-Gabbioneta srl. The authors are also grateful to Eng. Alessandro Pigoni and Eng. Lapo Galligani for the support provided.

REFERENCES

- Bakir F, Rey R, Gerber AG, Belamri T, Hutchinson B (2004). *Numerical and Experimental Investigations of the Cavitating Behavior of an Inducer*. International Journal of Rotating Machinery 10:15–25.
- Brennen CE (1994) *Hydrodynamic of Pumps*. Concepts ETI, Inc. and Oxford University Press
- Delannoy Y, Kueny JL (1990). *Two Phase Flow Approach in Unsteady Cavitation Modelling*. ASME-FED 98:153-158
- Dupont P (1991). *Etude de la Dynamique d'une Poche de Cavitation Partielle en vue de la Prediction de l'erosion dans les Turbomachines Hydrauliques*. PhD thesis, These No. 931, EPFL – Lausanne
- Kunz FK, Boger DA, Stinebring DR, Chyczewski TS, Gibeling HJ, Venkateswaran S, Govindan TR (1999). *A Preconditioned Navier Stokes Method for Two-Phase Flows with Application to Cavitation Prediction*. AIAA Paper no. AIAA-99-3329
- Marini A, Salvadori S, Bernardini C, Insinna M, Martelli F, Nicchio A, Piva A. (2011). *Numerical Prediction of Cavitation Inception in Centrifugal Impellers*. 9th European Turbomachinery Conference, 21-25 March 2011, Istanbul, Turkey, Paper No. ETC2011-214
- Menter FR (1992). *Improved Two-Equation k-ω Turbulence Models for Aerodynamic Flows*. Technical Report, NASA Technical Memorandum 103975

- Salvadori S, Cappelletti A, Martelli F, Nicchio A, Carbonino L, Piva A (2012). *Numerical Prediction of Cavitation in Pumps*. 15th International Conference on Fluid Flow Technologies CMFF'12, September 4-7, Budapest, Hungary, paper n. 173
- Singhal AK, Li HY, Athavale MM, Jiang Y (2001). *Mathematical Basis and Validation of the Full Cavitation Model*. ASME FEDSM 2001, New Orleans, Louisiana, USA
- Schnerr GH, Sauer J (2001). *Physical and Numerical Modeling of Unsteady Cavitation Dynamics*. 4th International Conference on Multiphase Flows, New Orleans, Louisiana, USA
- Stirling TE (1982). *Analysis of the Design of Two Pumps using NEL Methods*. Centrifugal Pumps Hydraulic Design, IMeche Conference Publications 183/82
- Tamura Y, Matsumoto Y (2009). *Improvement of Bubble Model for Cavitating Flow Simulations*. J. Hydrodynamics 21(1):41-46
- Tuzson, J (2000). *Centrifugal Pump Design*. Wiley-Interscience
- Yakhot V, Orszag SA, Thangam S, Gatski TB, Speziale CG (1992). *Development of Turbulence Models for Shear Flows by a Double Expansion Technique*. Physics of Fluids A, 4(7):1510-1520
- Zwart PJ, Gerber AG, Belamri T (2004). *A Two-Phase Flow Model for Predicting Cavitation Dynamics*. Proc. of 5th International Conference on Multiphase Flows, Yokohama, Japan